THE ASTROPHYSICAL JOURNAL, 474:490–495, 1997 January 1

REEXAMINATION OF COSMIC-RAY COMPOSITION AROUND 10^{18} eV FROM FLY'S EYE DATA

L. K. DING, C. L. JING, G. R. JING, J. L. REN, AND Q. Q. ZHU
Institute of High-Energy Physics, Chinese Academy of Sciences, Beijing, 100039, China
AND
H. Y. DAI, E. C. LOH, P. SOKOLSKY, P. SOMMERS, AND J. K. K. TANG
Institute of High-Energy Astrophysics, University of Utah, Salt Lake City, UT 84112
Received 1996 April 15; accepted 1996 July 18

ABSTRACT

The cosmic-ray composition around 10^{18} eV is reexamined using the Chou-Yang model for the simulation of air showers and comparing with Fly's Eye data. This model is quite different from models previously used. Using this model leads to the same conclusion that the primary cosmic-ray composition gets lighter in the region from 3×10^{17} eV to 10^{19} eV. This conclusion of a changing composition is not sensitive to the choice of model because it results from the measured elongation rate being greater than that predicted for a constant composition by any reasonable model that can account for the measured depths of shower maxima at the Fly's Eye threshold energy. That constraint on elongation rate for a constant composition also implies that the increased rate of energy dissipation that appears in hadron-nucleus interactions near 10^{14} eV may continue up to the region of 10^{19} eV.

Subject headings: cosmic rays — instrumentation: detectors

1. INTRODUCTION

The Fly's Eye experiment measures the longitudinal shower profile by observing the fluorescence light produced by cosmic-ray showers with energy above 10^{17} eV (Baltrusaitis et al. 1985a, 1985b; Cassiday 1985; Cassiday et al. 1990; Bird et al. 1993). It has been the only experiment to measure directly the longitudinal profile of air showers, thus providing valuable data for studies of the development and attenuation behavior of air showers induced by the highest energy cosmic rays. This behavior is commonly recognized to be closely related to the primary cosmic-ray composition as well as to the properties of hadronic and nuclear interactions in the corresponding energy region.

The chemical composition of primary cosmic-ray nuclei is very important for the study of the production, acceleration and propagation of cosmic rays. Direct composition measurements in space can only reach the energy region of a few times 10^{14} eV per particle (Burnet et al. 1990; Muller et al. 1991; Ichimura et al. 1993) because they are limited by the detector acceptance and low flux of high-energy cosmic rays. In the higher energy region all our knowledge of the composition (and spectrum as well) is deduced indirectly from the observation of air showers on the ground. In fact, the longitudinal development of high-energy air showers is determined by many physics factors. Among these are the species of incident particle, the inelastic cross section of high-energy hadron-air nucleus (h-air) collisions, and the energy dissipation properties of the inelastic h-air interactions. Therefore, any inferred conclusion about composition will depend on the particle interaction model applied in simulating the air showers. Looking at the situation in the lower energy region from 10^{14} to 10^{17} eV, a commonly accepted fact is that there is a "knee" in the cosmic-ray total particle spectrum between 10^{15} and 10^{16} eV. Such a change of the energy spectrum is considered to be related to a change of composition that may depend on the acceleration and confinement mechanism of cosmic rays in the Galaxy. However, up to the present time the composition in the knee region has been an open problem. For example, in the studies of gamma-ray families observed by mountain emulsion chambers different conclusions on composition in the energy region from 10^{14} to 10^{17} eV have been reported, as a result of using different interaction models (Lattes et al. 1980; Amenomori et al. 1982; Shibata 1981; Ren et al. 1988; Baradzei 1992; Zhu et al. 1990).

The energy spectrum and composition above 10^{17} eV are also important because they may relate to the existence of extragalactic cosmic-ray sources, which are believed to have an elemental composition significantly different from that observed at lower energies. In the paper by Gaisser et al. (1993), the KNP model and minijet model (both characterized by increasing inelasticity) were used to analyze the Fly's Eye data and it was concluded that the fraction of protons appears to increase in the highest explored energy region.

The aim of this work is to examine the robustness of the above conclusion on composition by using a different interaction model. It is necessary to see whether the situation is similar to that in the "knee" region or if the profile measurement can improve on it. If the above composition conclusion could be shown not to depend on the interaction model, it will be established on a firmer basis and have significant implications for cosmic-ray physics and astrophysics.

The motivation for using a different model is the following: The problem of how the inelasticity changes with energy has been an unsolved problem. It is noticed that at energies higher than the ISR ($s^{1/2} = 63$ GeV) hadron collider experiments have not been able to measure particles produced in very forward regions, which include leading particles and large x (Feynman variable) particles. Therefore, no direct experimental indications are available to show how the inelasticity changes with energy and what the x distribution of particles produced in the fragmentation regions should be. Furthermore the successful strong interaction theory, QCD, is not able to tell us the behavior of

particles produced in the very forward region because this is related to soft interactions. Thus, one can only rely on phenomenological models to analyze cosmic-ray data that, because of the lack of accelerator data for calibration, predict very different behavior in the forward region and very different energy dependence for the inelasticity. Therefore, it is useful for the composition study to examine the effect of another kind of model that has a different behavior in the forward region.

In this paper we adopt a decreasing inelasticity model in contrast to ones previously used. We reanalyze the depth of average shower maxima versus energy measured by the stereo Fly's Eye detector to study its effect on the deduction of cosmic-ray composition. In § 2 the hadron-hadron, hadron-nucleus, and nucleus-nucleus interaction models are described. In § 3, we will briefly introduce the experimental data used and the way the Monte Carlo data are generated. Results are reported in § 4, and the conclusions are presented in § 5.

2. THE MODEL

2.1. *Hadronic Interaction Model*

In this work we will use the Chou-Yang model (Chou et al. 1985; Chou & Yang 1985) to describe the hadron-nucleon interaction up to 10^{20} eV. The basic assumption of this model is that the partition of energy into secondary particles on each side of the center of mass system of hadron collisions is a stochastic process. This process is governed by: (1) the requirement that the total energy of all secondary particles on each side be $E_0 \times h$ (where E_0 is the incident energy and h is the inelasticity in the center of mass system), (2) the transverse momentum cutoff factor $g(P_t)$, (3) the Bloch-Nordsieck factor d^3p/E and (4) correlation effects between particles. The simplest stochastic distribution for a single particle on each side, not taking into account effect (4), is

$$d^3n = K(d^3p/E)g(P_t) \exp(-E/T_p) .$$

The single particle inclusive distribution is

$$E\frac{d^3n}{d^3p} = Kg(P_t) \exp\left(\frac{-E}{T_p}\right),$$

where T_p is called the partition temperature, $g(P_t)$ is assumed by the authors to be an exponential function $\exp(-\alpha P_t)$, and K is a normalization constant related to the mean multiplicity of secondary particles. Since it does not use the parton picture, this model is mainly concerned with the statistical behavior of particle production and energy partition and has been shown to describe collider data well (Chou et al. 1985; Chou & Yang 1985; Ding et al. 1988). In addition, this model has a simple mathematical formulation, few adjustable parameters, and is easy to extrapolate to higher energies.

Using the experimentally reported pseudorapidity distributions at $s^{1/2} = 53$, 200, 540, and 900 GeV, the mean multiplicity and the mean transverse momentum for minimum bias events and in some pseudorapidity intervals (Alner et al. 1986, 1987), we determined the parameters α, T_p, and K, and the results are listed in Table 1. We show the resultant pseudorapidity distributions of the model calculation in Figure 1 with curves and compare with the data from UA5 (Alner et al. 1986, 1987). Good agreement between model and data is seen.

TABLE 1

PARAMETERS α, T_p, AND K

	$\sqrt{s}$			
PARAMETER	53 GeV	200 GeV	540 GeV	900 GeV
α (GeV^{-1})	4.55	4.40	4.24	4.15
T_p (GeV)	3.80	9.12	16.6	22.4
K (GeV^{-2}).....	13.0	14.6	16.0	16.8

In order to apply this model for our purpose we need to extrapolate it from $s^{1/2} = 10^3$–10^6 GeV. It is obvious that any extrapolation will inevitably have some arbitrariness. We perform a smooth extrapolation as follows:

1. We keep the naturally decreasing trend of α shown at lower energies. This means that $\langle P_t \rangle$ is continuously increasing with energy following a logarithmic law, though P_t is not important for a one-dimensional simulation.
2. T_p is taken to increase with energy approximately following a power law as shown at lower energies.
3. K is normalized to the mean multiplicity. In the accelerator energy region, both a logarithm squared law and a power-law fit the experimental mean charged multiplicity well. At higher energy, the latter predicts much higher $\langle n_{\rm ch} \rangle$-values than the former. The latter form leads to better agreement with the data (Gaisser et al. 1993) and leads to

$$\langle n_{\rm ch} \rangle = 3.34\sqrt{s}^{0.32} ,$$

where $s^{1/2}$ is in GeV.

The parameters α, T_p, and K for higher energies are then determined and listed in Table 2.

Taking the parameters determined above we calculate the inelasticity and x distribution analytically. The following properties of this model are shown:

1. The mean inelasticity decreases with energy.
2. The x distribution steepens when the energy increases, showing violation of Feynman scaling in both the central region and the fragmentation region.

We then build the corresponding Monte Carlo event generator. The details of the method used for the Monte Carlo code were given by Ding et al. (1988). The pseudorapidity

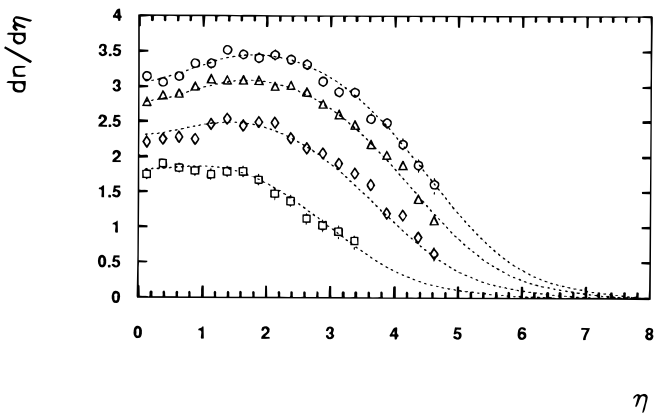

FIG. 1.—Pseudorapidity distributions for $p - p$ and $p - \bar{p}$ interactions. Data are from UA5 (Alner et al. 1986; 1987) for inelastic events with $s^{1/2} =$ 53, 200, 540, and 900 GeV expressed by squares, diamonds, triangles, and circles, respectively. Curves are results of the model calculation of this work.

TABLE 2

EXTRAPOLATION OF α, T_p, AND K, AND RESULTANT MEAN INELASTICITY

$\sqrt{s}$ (GeV)	α (GeV^{-1})	log T_p (T_p in GeV)	K (GeV^{-2})	$\langle h \rangle$
1800	4.02	1.54	17.7	0.295
4000	3.87	1.77	18.5	0.255
9000	3.68	2.00	19.7	0.219
18000	3.48	2.20	20.5	0.202
40000	3.25	2.45	21.2	0.189
90000	3.00	2.69	21.7	0.174
180000.....	2.77	2.89	21.9	0.162
400000.....	2.50	3.15	21.5	0.159
900000.....	2.21	3.42	20.4	0.156

distribution, inelasticity, x, and $\langle P_t \rangle$ distributions obtained by the code are in good agreement with the results of the numerical calculations. The average inelasticity in the laboratory system given by the generator is listed in the last column of Table 2.

2.2. *Hadron-Nucleus Interaction*

In real air showers, particles interact with air nuclei. Therefore, the inelastic cross section, inelasticity, and multiplicity of hadron-nucleus (h-A) interactions significantly influence shower development.

Adopting Glauber's theory on multiple diffraction scattering (Glauber & Matthiae 1970) one may derive the h-A cross section from the hadron-nucleon (h-N) cross section. We note that in the energy region of the Fly's Eye experiment the value of the h-N cross section is unknown. An additional uncertainty appears in the nucleon distribution of the air nucleus. We therefore intend to use an input h-A inelastic cross section and then vary it to evaluate its effect.

It is known that there may be more than one nucleon of the target nucleus wounded in an h-A inelastic collision. Consequently, there are more secondary particles produced and the inelasticity is larger than for h-N collisions at the same energy. Therefore, as emphasized by Gaisser (1992) and Fletcher et al. (1994), appropriately modeling the nuclear target in the shower simulation is important since it will significantly affect shower development. Accelerator data on h-A interactions are only available up to a few hundred GeV. We do not know in the higher energy region how large the nuclear target effects should be. In order to check the nuclear target effects we will consider two extreme cases. First we determine the number of wounded nucleons, ν, in a h-A collision by a Monte Carlo taking into account the nuclear collision geometry (Ding et al. 1990), which is well tuned by low-energy data where both h-N and h-A cross sections are measured. It is reasonable to assume that the nucleus geometry does not change with energy of the incident hadrons. However, the value of $\langle \nu \rangle$ and the ν distribution will change with energy due to the increasing h-N inelastic cross section.

In the first approach to h-A collisions we treat the h-A interaction as the superposition of ν independent h-N interactions. For each h-N interaction the leading hadron takes the energy fraction determined by the elasticity distribution given by the model. This approach obviously induces a strong nuclear target effect, hence a strong energy dissipation by the h-A collisions.

In the second approach, based on the dual parton model (DPM) (Capella & Tran Tranh Van 1981; Capella et al. 1985), ν intranuclear hadron-nucleon collisions are treated as one normal hadron-nucleon collision plus ν-1 collisions between a sea-quark of the projectile and a constituent quark of the target. As another extreme case, this approach has less energy dissipation and leads to a slower shower development. In the accelerator energy region both approaches roughly describe the data. But in the energy region we are concerned with the difference between them becomes much more apparent.

2.3. *Nucleus-Nucleus Interaction*

For the case of an incident nucleus the superposition model is always used. Here an incident nucleus A interacting with the target air nuclei is treated as the superposition of A nucleons independently interacting with air nuclei. We also use the successive fragmentation model (Zhu et al. 1990) in which the "A-air" cross section and the fragmentation probabilities of nucleus A and its fragments are taken into account. As shown later the differences in shower maxima as well as in elongation rates generated by these two models are very small.

3. EXPERIMENTAL AND SIMULATED DATA

The experimental data set used, the selection cuts and the reconstruction method are exactly the same as in Gaisser et al. (1993).

The Monte Carlo data are generated by a two-step simulation as in Gaisser et al. (1993). The first step is the air shower simulation using the interaction model introduced in the last section and taking an E^{-3} differential energy spectrum for incident cosmic rays. For an acceptable computation speed we parameterize hadronic showers with energy lower than 150 TeV by fitting the Monte Carlo results that were obtained by the simulation using the same code. For electrons with energy lower than 100 TeV and photons lower than 10 TeV the Greisen formula (Greisen 1960) is used to calculate the electron number at different depths.

The second step is the detector simulation, which uses the shower profiles provided by the first simulation as the input, generates them randomly in direction, zenith angle, and impact distance to the detector, models the produced fluorescence and Cherenkov light, propagates the light through the atmosphere, and determines the response of the detector taking into account the trigger condition. Thus, a fake event sample is produced. Taking the same cuts and reconstructing the fake event sample the same way as the real data, we may then compare them fairly. The details, as well as a discussion of possible systematic differences between real and fake data, are described in Gaisser et al. (1993).

4. RESULTS

We first generate a sample of showers using this code for the case of incident electrons. The resultant dependence of $\langle X_{\max} \rangle$ on log E is seen in Figure 2 with open circles and the fitted curve shows a constant elongation rate (which is defined as $d\langle X_{\max} \rangle / d \log E$; Linsley 1977; Linsley & Watson 1981) of 85.6 ± 0.3 g cm^{-2} for all energies, in agreement with theoretical expectation (85 g cm^{-2}) (Greisen 1960). This serves as a consistency check for our simulation.

We then simulate the case of pure proton and pure iron incidence taking $\sigma^{\rm inel}_{p-\rm air} = 290E^{0.04}$ (mb, and E in TeV) and $\sigma^{\rm inel}_{p-\rm air} = 290E^{0.06}$ and using the multi-interaction approach

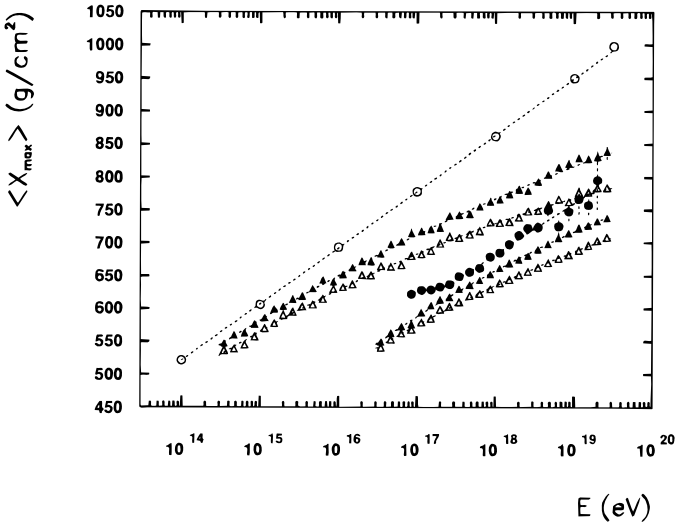

FIG. 2.—$\langle X_{max} \rangle$ vs. log E. Solid circles are Fly's Eye data (Gaisser et al. 1993). Open circles are simulation results for pure electromagnetic showers. Solid triangles are from simulation using model 4-1 and open triangles using model 6-1 (see text), and upper points are for incident protons, while lower points are for iron. The curves are fitted by a $\log^2 E$ law.

for h-air interactions. Hereafter, we abbreviate these as model 4-1 and model 6-1, respectively. These results are also shown in Figure 2 by solid triangles for model 4-1 and open triangles for model 6-1 (upper points are for proton incidence and lower points are for iron). The data (*solid circles*) are also drawn in the same figure for a preliminary comparison, though the detection efficiency has not been applied to the fake data in that figure. The following features are seen:

1. The fitted curves of $\langle X_{max} \rangle$ versus log E for both incident proton cases are lower than that of electrons in the whole energy region calculated. This is natural, since hadronic showers should produce an earlier mean shower maximum than pure electromagnetic showers at the same energy. Otherwise, the hadronic interaction model used would not be a reasonable one.

2. Starting from the energy region of 10^{14} eV the elongation rate of hadronic showers decreases continuously and gradually with energy as seen from the curves in Figure 2. The relation of $\langle X_{max} \rangle$ versus log E can be well fitted by a $\log^2 E$ law. As first shown by Linsley, the elongation rate for hadronic showers is always less than that of pure electromagnetic showers (Linsley 1977; Linsley & Watson 1981). Here we further show a log E dependence of the elongation rate, which is the result of the smooth change of certain physics quantities with energy. In the present simulation these include the power-law increase of the h-A inelastic cross section, the mean multiplicity, enhanced scaling violation, and enhanced nuclear target effects. The values of the elongation rates for model 4-1 and model 6-1 at different energies are listed in Table 3.

3. For the case of incident iron the fitted curve to the simulation result, which uses the successive fragmentation model for nucleus-nucleus collisions, is very close to what one gets by shifting the corresponding proton curve along the log E axis by log A ($A = 56$), indicating that the showers generated by the successive fragmentation model are very close to what would be given by the superposition model. The difference in $\langle X_{max} \rangle$ is shown by our calculation to be within 2%.

For the case of using the sea-quark approach for h-A interactions an obviously slower shower development is seen. The results (taking $\sigma^{inel}_{p-air} = 290E^{0.06}$; model 6-2) are plotted by open squares in Figure 3. The curves for incident electrons and for the data are also plotted in the same figure for comparison. The elongation rates of model 6-2 are also listed in Table 3. It is seen that for model 6-2 the value of $\langle X_{max} \rangle$ is about 60 g cm^{-2} larger at 10^{17} eV and about 90 g cm^{-2} larger at 10^{19} eV than that of model 6-1. In spite of the larger values of $\langle X_{max} \rangle$ all other features of model 4-1 and model 6-1 discussed above also exist for this case.

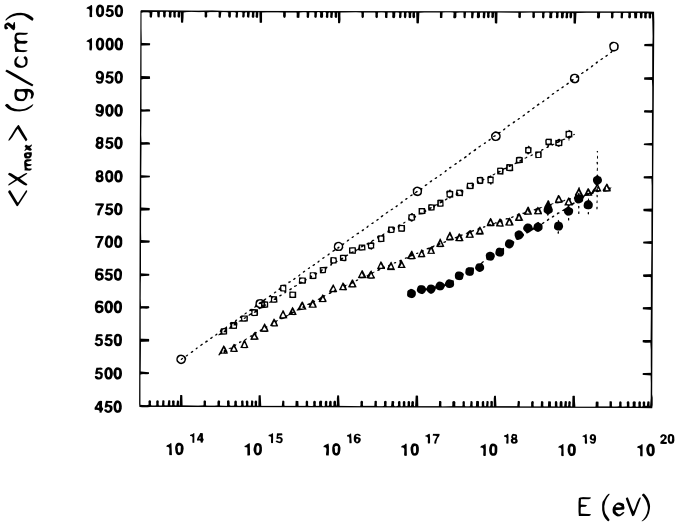

FIG. 3.—$\langle X_{max} \rangle$ vs. log E. Solid circles are Fly's Eye data (Gaisser et al. 1993). Open circles are simulation results for pure electromagnetic showers. Open squares and triangles are from simulations for incident protons using model 6-2 and model 6-1 (see text), respectively.

TABLE 3

CALCULATED ELONGATION RATES FOR DIFFERENT MODELS (VALUES IN PARENTHESES ARE AFTER DETECTOR SIMULATION)

	E				
MODEL	10^{15} eV	10^{16} eV	10^{17} eV	10^{18} eV	10^{19} eV
p: model 4-1	71.4 ± 0.65	65.1 ± 0.69	58.8 ± 0.72	52.4 ± 0.75	46.1 ± 0.78
Fe: model 4-1.....			76.4 ± 0.30	65.2 ± 0.32	53.9 ± 0.34
p: model 6-1	67.7 ± 0.60	59.3 ± 0.63	51.0 ± 0.66	42.6 ± 0.69	34.3 ± 0.72
			(53.5 ± 0.79)	(42.9 ± 0.83)	(32.3 ± 0.87)
Fe: model 6-1.....			65.0 ± 0.25	56.4 ± 0.27	47.7 ± 0.28
			(57.4 ± 0.71)	(48.3 ± 0.74)	(39.1 ± 0.78)
p: model 6-2	76.0 ± 0.94	71.3 ± 0.98	66.7 ± 1.0	62.0 ± 1.0	57.4 ± 1.1

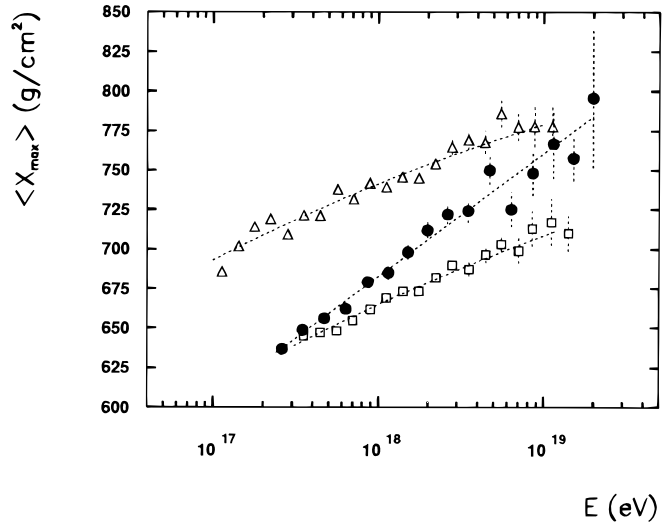

FIG. 4.—$\langle X_{max} \rangle$ vs. log E of model 6-1 after detector simulation. Solid circles are Fly's Eye data (Gaisser et al. 1993). Triangles are for incident protons, and squares are for iron. Curves are results from $\log^2 E$ fits.

These results show that beyond 10^{17} eV all models used above give an elongation rate of proton showers obviously smaller than that derived from the Fly's Eye data (79 ± 3 g cm^{-2}). From this feature alone we can say that these models also lead to the conclusion that the fraction of light nuclei in the primary cosmic rays increases from 3×10^{17} eV to 10^{19} eV, if the detector simulation does not change the elongation rate much.

We perform the detector simulation and compare the results with the Fly's Eye data from 3×10^{17} to 10^{19} eV. Figure 4 shows the result for model 6-1. It is seen that the detector simulation shifts the results of the model simulation up a little for proton showers and somewhat more for iron showers. After the detector simulation we can still fit the results by a $\log^2 E$ law as shown by curves in Figure 4. It is seen that model 6-1 is well suited to interpret Fly's Eye data. Table 3 lists in parentheses the elongation rates of model 6-1 after detector simulation. These are changed slightly but are still obviously lower than that of data.

After detector simulation the pure iron curves for model 4-1 and model 6-2 intercept the data curve. They should thus be ruled out since they induce too slow a shower development with respect to the Fly's Eye data. In order to fit the data using the sea-quark approach (*h-A* collisions incorporated with the *h-N* interaction model used in this work), we need to significantly speed up the shower development. If this is to be done by increasing the cross section we should take $\sigma^{\rm inel}_{p-{\rm air}} = 290E^{0.09}$ (model 9-2). Figure 5 shows the curves of $\sigma^{\rm inel}_{p-{\rm air}} = 290E^{\delta}$ with different δ-values. The measured cross sections reported by Akeno (*solid circles*) (Hara et al. 1983) and Fly's Eye (*open circle*) (Baltrusaitis et al. 1985a) are also shown in this figure. It is seen that $\delta = 0.09$ seems to be located in a region that is not acceptable.

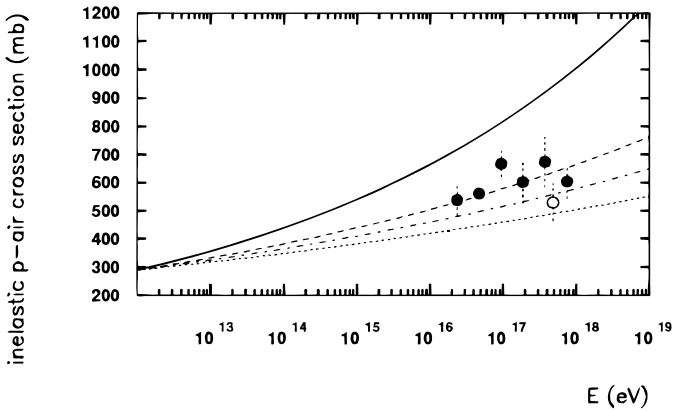

FIG. 5.—$\sigma^{\rm inel}_{p-{\rm air}} = 290E^{\delta}$ with $\delta = 0.04$, 0.05, 0.06, and 0.09 expressed by dotted, dot-dashed, dashed, and solid line, respectively. The measured cross sections are shown by open circle for the Fly's Eye experiment, and solid circles are for Akeno (Hara et al. 1983).

5. CONCLUSION AND DISCUSSION

As mentioned above, if the elongation rate for showers induced by a single species of nuclei in the energy region from 3×10^{17} to 10^{19} eV are smaller than the value from the Fly's Eye data, the composition of primary cosmic rays must be changing in the corresponding energy region toward an increasing fraction of light nuclei. We simulate the high-energy cascades in the air using the Chou-Yang model, which is characterized by decreasing inelasticity and scaling violation, and incorporate an increasing cross section and different *h-A* interaction approaches. All give rise to decreasing elongation rates that, in the energy region above 10^{17} eV, are smaller than the rate deduced from data. This shows that the models with decreasing inelasticity lead to a conclusion on the change of the composition around 10^{18} eV, which is qualitatively the same as the conclusion deduced using the models with increasing inelasticity (Gaisser et al. 1993).

Thus, this qualitative conclusion is not sensitive to the choice of interaction model. Essentially, this model independence comes from the following facts: the elongation rate observed by the Fly's Eye (79 ± 3 g cm^{-2}) is rather large, close to that expected for pure electromagnetic showers (about 85 g cm^{-2}), and the value of the observed mean shower maxima above 3×10^{17} eV is small, about 180 g cm^{-2} smaller than that for pure electromagnetic showers at the same energy. For the case of a single nuclear species (for example, for incident protons) any interaction model that gives an appropriate shower development having a value of $\langle X_{max} \rangle$ as low as the Fly's Eye data requires, must involve some increasing energy dependences in some physics quantities. Increasing cross section, increasing multiplicity, increasing inelasticity, enhanced scaling violation and enhanced *h-A* interactions are examples of possible quantities. One must involve most of these factors in models in order to get the shallower shower maxima. Thus, these models inevitably lead to an elongation rate (for any constant composition) that decreases gradually with energy and is smaller than the value given by the data in the Fly's Eye energy region.

In other words, the measurement of the absolute depth of shower maxima together with the elongation rate brings us information on the composition, which is not contaminated by uncertainties arising from different interaction models.

It should be noted here that the above conclusion is based on the assumption of a smooth extrapolation of hadronic interaction properties. The situation would be different if there were a sudden change of interaction properties at some energy.

The elongation rate as well as the values of $\langle X_{max} \rangle$ from the Fly's Eye data also provide constraints on the hadronic and nuclear interactions in the energy region above 10^{17} eV.

In addition, pure electromagnetic showers bound $\langle X_{\max} \rangle$ from above. Thus, those models that generate too slow a shower development make the curve for incident protons intercept or lie above the electron curve, or they make the curve for incident iron nuclei intercept or lie above the data curve. Models that generate too fast a shower development make the curve for incident protons intercept or lie under the data curve. The Fly's Eye data can be used to rule out classes of models by such comparisons.

From the above analysis it is shown that, to fit the Fly's Eye data, quantities having strong energy dependence are necessary in the models. They will have a global effect of increasing the energy dissipation rate. In fact the decrease of the elongation rate with energy shown in this work is a continuation of the well known rapid development and attenuation of high-energy showers observed by different kinds of cosmic-ray experiments above 10^{14} eV (Lattes et al. 1980; Amenomori et al. 1982; Shibata 1981; Ren et al. 1988; Baradzei 1992; Zhu et al. 1990). What the Fly's Eye data tell us is that this trend of the energy dissipation rate increasing with energy continues up to 10^{19} eV.

L. K. D. and J. L. R. are grateful to E. C. Loh for his invitation and to all the members of Fly's Eye group for their hospitality during their stay at the University of Utah. Thanks of L. K. D. go to G. J. Wang and A. Tai for helpful discussions and to Y. D. He for comments of the draft. The authors appreciate the support obtained from the Utah Supercomputing Institute. Without it this calculation could not be completed. This work is supported by US NSF and Chinese Academy of Sciences as the implementation of a project of US-China Cooperative Science Program.

REFERENCES

Alner, G. L., et al. 1986, Z. Phys. C, 33, 1
———. 1987, Nucl. Phys. B, 291, 445
Amenomori, M., et al. 1982, Phys. Rev. D, 25, 2807
Baltrusaitis, R. M., et al. 1985a, Phys. Rev. Lett., 52, 1380
———. 1985b, Nucl. Instrum. Meth. Phys. Res., 240, 410
Baradzei, L. T. 1992, Nucl. Phys. B, 370, 365
Bird, D. J., et al. 1993, Phys. Rev. Lett., 71, 3401
Burnet, T. H., et al. 1990, ApJ, 349, 25
Capella, A., & Tran Tranh Van, J. 1981, Z. Phys. C, 10, 249
Capella, A., et al. 1985, Phys. Rev. D, 32, 2933
Cassiday, G. L. 1985, Ann. Rev. Nucl. Part. Sci., 35, 321
Cassiday, G. L., et al. 1990, ApJ, 356, 669
Chou, T. T., et al. 1985, Phys. Rev. Lett., 54, 510
Chou, T. T., & Yang, C. N. 1985, Phys. Rev. D, 32, 1692
Ding, L. K., et al. 1988, High Energy Phys. Nucl. Phys., 12, 731
Ding, L. K., et al. 1990, High Energy Phys. Nucl. Phys., 14, 219
Fletcher, R. S., et al. 1994, Phys. Rev. D, 50, 5710
Gaisser, T. K. 1992, Nucl. Phys. B, 28, 61
Gaisser, T. K., et al. 1993, Phys. Rev. D, 47, 1919
Glauber, R. J., & Matthiae, G. 1970, Nucl. Phys. B, 21, 135
Greisen, K. 1960, Ann. Rev. Nucl. Sci., 10, 63
Ichimura, M., et al. 1993, Phys. Rev. D, 48, 1949
Hara, T., et al. 1983, Phys. Rev. Lett., 50, 2058
Lattes, C. M. G., et al. 1980, Phys. Rep., 65, 101
Linsley, J. 1977, Proc. 15th Int. Cosmic-Ray Conf. (Plovdiv), 12, 89
Linsley, J., & Watson, A. A. 1981, Phys. Rev. Lett., 46, 459
Muller, D., et al. 1991, ApJ, 374, 356
Ren, J. R., et al. 1988, Phys. Rev. D, 38, 1404
Shibata, M. 1981, Phys. Rev. D, 24, 1487
Zhu, Q. Q., et al. 1990, J. Phys. G, 16, 295